

Received April 19, 2021, accepted May 5, 2021, date of publication May 24, 2021, date of current version June 3, 2021.

Digital Object Identifier 10.1109/ACCESS.2021.3083067

Dynamic Analysis and Libration Control of Electrodynamic Tether for Reboost Applications

YANFANG LI^{1,2}, AIJUN LI¹, CHANGQING WANG¹, AND HAOCHANG TIAN¹

¹School of Automation, Northwestern Polytechnical University, Xi'an 710129, China

²College of Energy Engineering, Yulin University, Yulin 719000, China

Corresponding author: Yanfang Li (lyf2017@mail.nwpu.edu.cn)


This work was supported in part by the National Natural Science Foundation of China under Grant 51808447 and Grant 61803307, in part by the Natural Science Basic Research Plan in Shaanxi Province of China under Grant 2020JQ-209, and in part by the Science and Technology Bureau of Yulin City under Grant CXY-2020-007.

ABSTRACT Electrodynamic tethers can be employed as an immensely promising propulsion system for boosting the altitude of spacecraft, cite instance space stations, satellites, and the like, which ameliorates the expenditure of fuel and minimizes detrimental spacecraft impacts. This paper analyzes the libration dynamics and stability of reboost spacecraft with insulation electrodynamic tethers. A key aspect of spacecraft reboost with an electrodynamic tether is how to keep the tether aligned with the local vertical and stabilized in the context of external disturbances. It has been shown in the current research that the librational instability results in the tether slackness and swings in long-term motion without effective control. Moreover, electrodynamic force (Ampere force) is regarded as a distributed load acting on the tether causing tether deformations which may be detrimental if severe. Aiming at the problem, an optimal control method and PID are given to stabilize the libration motion by modulating the tether current. The dynamical model of the electrodynamic tether system is established using Lagrange equations of the second kind under considering tether deformation and control laws are proposed based on the model. The effectiveness of libration stability control is validated through numerical results in which a current regulation law with appropriate control parameters is used for the libration motion of electrodynamic tether system.

INDEX TERMS Electrodynamic tether, spacecraft reboost, tether deformation, dynamic analysis, libration control.

I. INTRODUCTION

Lower mission cost has been considered as one of the keys to the exploitation and exploration of space. On this count, several “free force” applications will naturally bring to mind once the traditional paradigm of chemical propulsion and expensive space launch is replaced by the electrodynamic tether (EDT) concept [1]. The EDT system is a new type of space vehicle, which has been paid great attention and emphasis and has composed of two or more spacecrafts (like satellites) and a long conductive tether. The current flowing within the tether will interact with the Earth's magnetic field such that the orbit and altitude of the system can be altered utilizing the resulted electrodynamic force (ED force) without the expenditure of propellant. The EDT system can widely be employed in space exploration and exploitation [2], [3].

The associate editor coordinating the review of this manuscript and approving it for publication was Halil Ersin Soken .

Two key applications of the EDT system are those of reboost and deorbiting [4]–[6].

As an example of reboost Chinese Space Station (CSS), this paper makes research on the kinematics and dynamics analysis and libration motions control of the EDT system. Similar examples can also be found in literature, the International Space Station (ISS) reboost with an EDT [7]. Although the mission to rescue the ISS with the EDT was never accomplished, we learned a lot about EDT while it worked, especially libration dynamics in tether and multi-resonance in ISS, and finding simple methods to stabilize those motions is a particularly challenging issue.

It is well known that the CSS has a broad cross-sectional area and orbits at a relatively low orbital altitude (370km), which requires periodic reboost due to the atmospheric drag acting on it. Traditionally, the tasks of reboost are achieved utilizing rockets/thruster, yet they are not economical. The ED force generated by the conductive tether motion in the

Earth's magnetic field can be seen as an ion thruster that provides the power to adjust the orbit altitude. Comparatively, the advanced EDT technology has distinct advantages in reboost of the CSS for its structural simplicity, high efficiency, low cost, and easy operation [8]. However, the ED force is a double-edged sword, which is regarded as a distributed load acting on the tether, causing not only in-plane and out-of-plane libration motions but also induced tether deformation, which can arouse tether slackness and swings without effective control. What this means is that careful control of the electric current of the tether is indispensable to bring about expected changes to the CSS's orbital parameters. Therefore, an essential problem for the reboost applications is the dynamic stability of the EDT [9]–[12].

Plenty of researchers have made a big effort to the dynamic stability of the EDT system, and the relevant modeling, dynamic analysis, and libration motion control are studied. Generally, the dumbbell model was adopted to lighten the analysis and design controller while the multipoint model is used for dynamic analysis. For example, Xu and Kong established two different models in their paper, and it can be found that the dumbbell model has theoretical rationality, and the flexible cable model is more consistent with the natural characteristics of the EDT system [13]. Liu used an insulated EDT as an orbital boost maneuver system to analyze the libration dynamics of electrodynamic tethered satellite take into account coupled multiphysics model [14], [15]. Moreover, a multipoint model is used to verify the effectiveness of the control law designed by a rigid rod model [4]. As for the libration control issues, there are diverse control methods are presented from different perspectives. Such as Peláez, Iñárrrea, Kojima, Williams, Yang et. al. investigated the time-delay autosynchronization (TDA) method and extended time-delay autosynchronization (ETDA) method to stabilizing the libration motions of EDT in the circular orbit and elliptical orbit [9], [16]–[19]. The study of Zhong shows that the libration dynamics and stability of EDT system is a key issue and regulated electric current in the tether to stable the libration motions [20]. Luo and Chen have developed the libration motions of EDT system by regular the tether current and length during the tether deployment [21], [22]. Li used a high fidelity multiphysics model of the EDT system for libration and transverse motion control of the system [23]. Tikhonov proposed a device that creates active controlling dissipative moment and the construction of the damper used for keeping the EDT along the local vertical [24]. Although the cited techniques have proved to be valid, the tether deformation is not avoidable for an EDT system in the long run, yet it is ignored, and the relevant studies are relatively scarce.

The focus of this paper is on dynamic analysis and vibration control of the EDT system via the regulation of current along the tether, considering the tether deformation. The tether electric current is determined as the sum of the command current I_n (the given electric current) and the current corrections ΔI (the designed controller). Unlike many existing works on the libration stability control using a rigid rod

model (the tether is close to a straight line) to design the controller. The shape of the tether is projected into a circle arc (a part of a circle) in the orbit plane when the tether mass is not taken into consideration since the Ampere force is regarded as a distributed load acting on the tether [25]. However, a variation of the circular arc is represented the degree of tether bowing, which can result in the EDT system is unstable. To ensure stability and eliminate libration motion, an optimal control law based on the Bellman dynamic programming principle and PID are presented.

The organization of this paper is as follows. In section II, the dynamic modeling of the EDT system is established. Section III is devoted to the analysis of the dynamic of quasi-equilibrium positions. The proposed control laws are developed in Section IV. Simulation studies are conducted to evaluate the control performance in Section V. Finally, conclusions are drawn in Section VI.

II. DYNAMICS OF REBOOST EDT SYSTEM

A. EQUATION OF MOTION OF REBOOST EDT SYSTEM

A reboost EDT system is made of the CSS and subsatellite connected by a conductive tether in a geometric inertial coordinate system $OXYZ$ as shown in Figure 1. The subsatellite is equipped with a hollow cathode collector which is used for charge exchange with the space plasma environment. Because the tether length of the reboost EDT system is extremely small compared to the radius of the earth, one can model the reboost EDT system as a lumped mass located at the Center of Mass (CM) of the system in the orbital dynamic analysis.

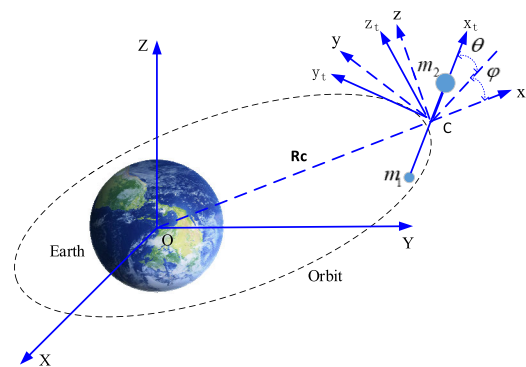


FIGURE 1. Coordinate systems.

The mathematical model of the reboost EDT system is established in the orbital coordinate system $Cxyz$. The position of the tether frame $Cx_1y_1z_1$ relative to the coordinate system $Cxyz$ is depicted by in-plane angle θ and out-of-plane angle φ , see in Figure 1. The equations of motion are derived using the Lagrange method of the second kind under considering tether deformation. In [25], [26], the dynamic equations of the EDT system related to the CM have been derived as

$$\begin{aligned} \ddot{r} - r[\dot{\varphi}^2 + (\dot{\theta} + \dot{\varphi})^2 \cos^2 \varphi + v^{-1} \dot{\varphi}^2 (3 \cos^2 \theta \cos^2 \varphi - 1)] \\ = \frac{Q_r}{m_e} \end{aligned} \quad (1)$$

$$\ddot{\theta} + \ddot{\varphi} + 2(\dot{\theta} + \dot{\varphi})\left(\frac{\dot{r}}{r} - \dot{\varphi} \tan \varphi\right) + 1.5\nu^{-1}\dot{\vartheta}^2 \sin 2\theta = \frac{Q_\theta}{m_e r^2 \cos^2 \varphi} \quad (2)$$

$$\ddot{\varphi} + 2\dot{\varphi}\left(\frac{\dot{r}}{r}\right) + [0.5(\dot{\theta} + \dot{\varphi})^2 + 1.5\nu^{-1}\dot{\vartheta}^2 \cos^2 \theta] \sin 2\varphi = \frac{Q_\varphi}{m_e r^2} \quad (3)$$

where, r is the distance of the two end-bodies (tether chord length), $m = m_1 + m_2$ is the total system mass, m_1 is the subsatellite mass, m_2 is the CSS mass; m_e is defined as the reduced mass of the system: $m_e = m_1 m_2 / m$; $\nu = 1 + e \cos \vartheta$, e is the orbital eccentricity; ϑ is the true anomaly; $\dot{\vartheta} = (K/p^3)^{0.5} \nu^2$, $\ddot{\vartheta} = -2Ke \sin \vartheta / p^3$; p is the orbital parameter; K is constant of gravitation; Q_r is a generalized force concerning for to the distance r , Q_θ and Q_φ are the generalized electrodynamic torques for the in-plane angle θ and out-of-plane φ act on the EDT system, respectively.

The Ampere force per unit length of the tether is

$$dF = I_n l \times B \quad (4)$$

where $l = (l_x, l_y, l_z)$ is the unit vector along the tangential direction of the tether, l_x, l_y, l_z are direction cosine in the orbital coordinate system $Cxyz$, I_n is a command current along the tether, and the tether current is assumed positive when it flows from the subsatellite to the CSS. $B = (B_x, B_y, B_z)^T$ is the geomagnetic induction vector in the orbital frame whose components can be expressed as (assuming a non-tilted dipole model) [27]

$$\begin{aligned} B_x &= -2B_0 \sin i \sin u \\ B_y &= B_0 \sin i \cos u \\ B_z &= B_0 \cos i \end{aligned} \quad (5)$$

where $B_0 = \mu_m / R_c^3$, μ_m is the magnetic moment of the Earth's dipole, R_c is the radius of the CM, i is the orbital inclination, u is the argument of the latitude.

Regardless of the tether mass and assuming that the shape of the tether is projected into a circle arc in the orbit plane under the action of Ampere force [25]. The generalized forces Q_r , Q_θ and Q_φ can be derived by the principle of virtual work, that is

$$Q_r = -0.5B_0 \cos i |I| r (\cot \psi \cos^2 \varphi + \psi^{-1} \sin^2 \varphi) \quad (6)$$

$$Q_\theta = B_0 I r \Delta \cos \varphi [\cos \varphi \cos i - \sin \varphi \sin i \sin(\theta + u)] + 3B_0 I r \Delta \cos \varphi \sin i \cos \theta \sin \varphi \sin u \quad (7)$$

$$Q_\varphi = 0.5B_0 \cos i |I| r^2 \sin \varphi \cos \varphi (\cot \psi - \psi^{-1}) + B_0 I r \Delta \sin i [\cos(\theta + u) + 3 \sin \theta \sin u] \quad (8)$$

where $\Delta = 0.5r(m_2 - m_1)/m$ is the distance from the point of application of the Ampere force to the CM. While ψ is angle between tether chord length and the tangent of the circle through the endpoint of the tether (tether deformation angle), which is depended upon the tether tension. That is

$$r = L\gamma / [\sin^2 \varphi + \cos^2 \varphi (\psi / \sin \psi)^2]^{0.5} \quad (9)$$

where L is undeformed tether length, $\gamma = 2E\psi / (2E\psi - B|I|L)$ is an elongation of tether (which obeys Hooke's Law), while E is the Young modulus.

The motion of the EDT system relative to the CM is described by equations (1-9) in the consideration of the tether deformation. It can be seen that if $e = 0$, $i = 0$ and $m_2 \gg m_1$, the equations (1-3) are consistent with the result of Ref. 26.

Assuming the EDTs runs in a circular orbit, to convenience analysis, the equations (1), (2), and (3) are further recast into the following dimensionless form

$$r'' - r[\varphi'^2 + (\theta' + 1)^2 \cos^2 \varphi + 3 \cos^2 \theta \cos^2 \varphi - 1] = \frac{Q_r}{m_e \Omega^2} \quad (10)$$

$$\theta'' + 2(\theta' + 1)\left(\frac{r'}{r} - \varphi' \tan \varphi\right) + 1.5 \sin 2\theta = \frac{Q_\theta}{m_e r^2 \cos^2 \varphi \Omega^2} \quad (11)$$

$$\varphi'' + 2\varphi'\left(\frac{r'}{r}\right) + [0.5(\theta' + 1)^2 + 1.5 \cos^2 \theta] \sin 2\varphi = \frac{Q_\varphi}{m_e r^2 \Omega^2} \quad (12)$$

by introducing the dimensionless transformations $(\)' = d(\)/d\tau$. In the above formulations, the derivative with respect to the dimensionless time $\tau = \Omega t$, and Ω is orbital angular velocity.

B. THE SELECTION OF EDT SYSTEM PARAMETERS

The electric current in the tether and the hollow cathode collector interacts with the Earth's magnetic field and generate the Ampere force distributed along the wire which causes the tether is bent out of shape and may even result in adverse effects if the bending is severe. At that point, beyond the above reason, the system parameters (such as tether length, electric current, the end-body mass, and so on) also affect how the tether changes, with suppose the tether tension is big enough to keep deformation small. And that is helpful in selecting the system parameters.

Next, the tether deformation was analyzed with different system parameters. The system initial conditions are provided in TABLE 1.

Case1: The tether current is set to be $-0.25A$, $-0.5A$, $-2A$, $-3A$, respectively.

Four case studies with a different electric current in the tether are proposed for comparison. The time of histories of the tether deformation angle ψ is shown in Figure 2 for the four cases. As seen in the figure, the dynamics response of the angle ψ with $I = -0.25A$ equal to zero and mutation at some point. It is indicated that the tether deformation angle is not a normal calculation with low current. In other words, the mathematical model of the EDT system is not applied to a low current. Similarly, the model is not employed when such deformation so much is caused by a big current $I = -3A$. Therefore, a suitable current value can be selected to obtain a normal deformation angle. A similar analysis is

TABLE 1. System parameters and initial conditions.

Symbol	Parameters	Values
m_1	Mass of subsatellite	50kg
m_2	Mass of the CSS	90000kg
H	Orbit altitude	400km
L	Tether length	2km
I	Tether current	-2A
e	Orbit eccentricity	0.0001
i	Orbit inclination	0.733/rad
θ_0, φ_0	Angle	0.35, 0.35/rad
$\dot{\theta}_0, \dot{\varphi}_0$	Angular velocity	0, 0 rad/s

Km = kilometer, A = ampere, kg = kilogram, S=second

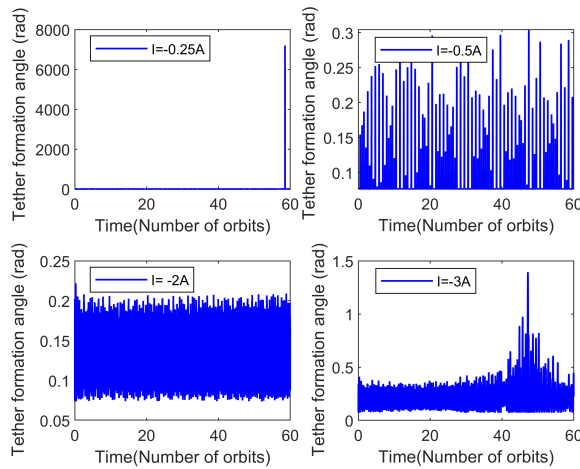


FIGURE 2. Variation curves of the deformation angle versus the electric current.

conducted with the current direction reversed. Based on the above analysis the tether current is selected -2A in this paper, which fulfills the request of the mission profile, and keeps the tether deformation calculates normally.

Case2: The tether length is set to be 1km, 2km, 3km, 3.6km, respectively.

Figure 3 depicts the time histories of the tether deformation angle with different tether lengths or the four cases. It can be seen from Figure 3 that the tether deformation angle ψ increases with an increase in tether length in the first three figures because the tether length is the more, the Ampere force is the bigger. While the fourth in Figure 3 the deformation angle is appeared abnormal at some point that may be caused by the large Ampere force. The dynamic model of the EDT system has failed in the circumstances. For practical applications, however, the reliability of the EDT system is a challenge under a too long tether. Here the chosen tether is 3km satisfied the reboost task requirements and also are references for the other space missions.

Case3: The mass of the subsatellite is set to be 50kg, 100kg, 200kg, 250kg, respectively.

Figure 4 indicates a difference between the profiles of the angle ψ with the different mass of subsatellite in the four cases. It can be found through a comparison of the first

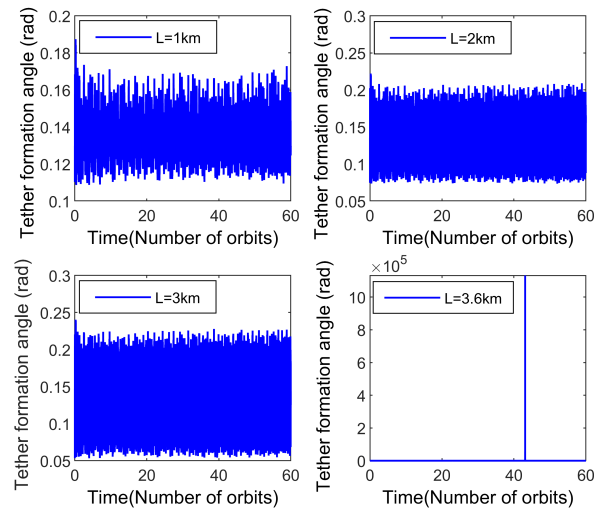


FIGURE 3. Variation curves of the deformation angle versus the tether chord length.

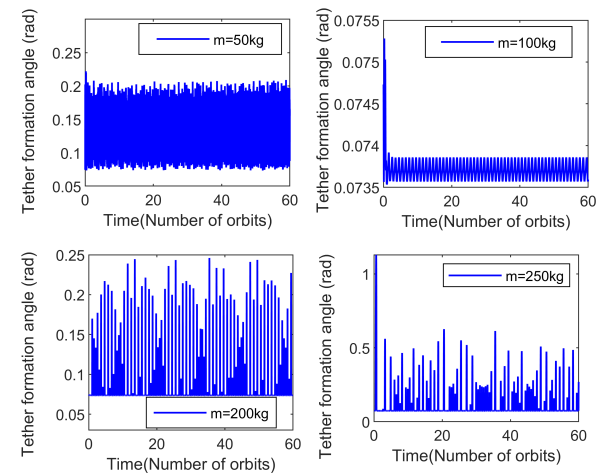


FIGURE 4. Variation curves of the deformation angle versus the mass of end-body.

three cases that the deformation angle is computed normally. The tether deformation is too large when the mass of the lower end-body is much than 250kg. A relatively small mass of end-body can minimize the impact on the CSS (the center of mass of the EDT system shift), so the subsatellite’s mass of 50kg is selected.

In conclusion, the EDT system model cannot be applied when the tether deformation angle is too big or too small (premises condition is assumed that the projection of the tether in the orbital plane is an arc of a circle).

III. THE QUASI-EQUILIBRIUM POSITIONS OF EDT SYSTEM

The equilibrium positions of the tether system in the orbit plane are the most concern from the point of practical engineering. It well known that when no electricity is flowing through the tether, the equilibrium positions of the system are existing and stable and when a small constant current flows the tether, the equilibrium positions are not existing

and unstable. The EDT system is forced libration around the proximate equilibrium positions (so-called quasi-equilibrium positions) at an angle. To facilitate analysis of the motion of the EDT system along an orbit, we should determine the quasi-equilibrium positions of the system in the orbit plane firstly. Orbit parameters and true anomaly ϑ are often assumed to be given when the quasi-equilibrium positions are solved. Suppose the orbit parameters are slow variables, and then the true anomaly has a very minimal impact on the motions of the EDT system, which is true in the case of the circular orbit (that is $e \approx 0$). Then the quasi-equilibrium positions of the EDT system are obtained from the equations (1)-(3). Take an equatorial plane (namely $i=0$) for example, setting $\dot{r} = \dot{\theta} = \dot{\varphi} = 0$ in (1)-(3) and denoting $T = Q_r$, $r = L$ (T is tether tension) when the tether is fully deployed.

A. QUASI-EQUILIBRIUM POSITIONS OF EDT SYSTEM

Based on the above assumptions, the quasi-equilibrium positions are determined from the equations (2):

$$1.5v^{-1}\dot{\vartheta}^2 \sin 2\theta = Q_\theta/m_e r^2 \cos^2 \varphi \quad (13)$$

Form equation (13), it can be obtained four quasi-equilibrium positions [26]:

$$\theta_1^* = \frac{1}{2} \arcsin(\delta) \quad \theta_2^* = \theta_1 + \pi \quad (14)$$

$$\theta_3^* = \frac{\pi}{2} \text{sign}(\delta) - \frac{1}{2} \arcsin(\delta) \quad \theta_4^* = \theta_3 + \pi \quad (15)$$

where $\delta = \mu_m(m_2 - m_1)I \cos(i)/3Km_1m_2 + 4e \sin \vartheta/3v^3$. It is worth noting that lots of factors influence the quasi-equilibrium positions of the system, including the electric current, eccentricity, the mass of end-body, orbital inclination, and the true anomaly.

At these quasi-equilibrium points, the deformation angle ψ and the chord length r in equations (1)-(3) are expressed by the following formulas

$$\begin{aligned} \psi_j &= \arctg\left(\frac{\mu_m |I|}{6Km_e \cos^2 \theta_j}\right), \quad r_j = L\gamma \frac{\sin \psi_j}{\psi_j}, \quad \dot{\theta}_j \\ &= \dot{r}_j = \dot{\varphi} = 0 \end{aligned} \quad (16)$$

when $|\delta|$ is sufficiently small, the quasi-equilibrium positions in the first group (14) are approached the local vertical and in the second group (15) are close to the horizontal. To ensure that the above quasi-equilibrium positions existence, the condition $|\delta| < 1$ must be satisfied. However, it is focused on the quasi-equilibrium positions are near the local vertical (14), due to the ED force is almost parallel to the direction of the velocity vector of the CM of the EDT system [25], [26].

The operating mode of the EDT system is dependent on the directions of the tether deployment and the tether current. In general, there are two operating modes: generation mode and thrust mode. In the generation mode, the EDT is tilted in the opposite direction of the orbital motion, while in the thrust mode, it is tilted in the direction of orbital motion [27]. In this paper, as mentioned, the tether is deployed downward

and the electric current flows from the subsatellite to the main satellite ($I < 0$, $\theta_1^* < 0$) so the EDT system is in thrust mode.

B. CALCULATION OF TETHER TENSION

At the quasi-equilibrium positions, the natural tension of tether is obtained from the equations (1):

$$T^* = m_e L [\dot{\varphi}^2 + (\dot{\theta} + \dot{\vartheta})^2 \cos^2 \varphi + v^{-1} \dot{\vartheta}^2 (3 \cos^2 \theta \cos^2 \varphi - 1)] \quad (17)$$

The allowable domain of the tension force is limited to be $0 < T < T^*$, where the bounds are set according to consideration that the tether must be kept taut and the force must be bounded for the practical application. The maximum tension in equation (17) is derived at the quasi-equilibrium positions and taken as a terminal condition of tether deployment. Yet, it is a rational approximation value based on the result of numerical calculation and considered an empirical value.

C. CRITICAL CURRENT AT QUASI-EQUILIBRIUM POSITIONS

For the case of a circular orbit, equation (13) may be rewritten as

$$1.5\dot{\vartheta}^2 \sin 2\theta = B_0 I \Delta / m_e L \quad (18)$$

Hence, the critical current is obtained as

$$I^* \approx 3Km_s \sin(2\theta) / \mu_m \quad (19)$$

where $m_s = m_1 m_2 / (m_2 - m_1)$.

Note that there is a maximum critical current that has existed when the quasi-equilibrium point is $\theta^* = \pm\pi/4 + n\pi$ (n can be an arbitrary integer), that is $|\sin(2\theta^*)| = 1$. By now the biggest tether critical current is expressed as

$$I_{\max}^* \approx 3Km_s / \mu_m \quad (20)$$

Equation (20) shows the maximum critical current to the mass distribution of the EDT system. It should be noted that if $m_1 = m_2$, I_{\max}^* will not exist and if $m_1 \neq m_2$, the mass of two end-bodies can vary much which is indicated that the range of allowable current is broadened.

IV. CONTROLLERS DESIGN

There are two control laws of current for the three-dimensional motion of the EDT system is devised to diminish the libration motions and tether deformation of the system. To ease the design of stabilizing control laws for the EDT system, the system of second-order nonlinear equations (10)-(12) can be arranged in state-space equations. The state-space form to be used in a control system that governs the behavior of r , θ and φ .

The system states are defined as $\mathbf{x} = (r, \dot{r}, \theta, \dot{\theta}, \varphi, \dot{\varphi})^T = (x_1, x_2, x_3, x_4, x_5, x_6)^T$. The equations of libration motion in the state-space form are given by

$$\begin{aligned} x_1' &= x_2 \\ x_2' &= x_1 [x_6^2 + (x_4 + 1)^2 \cos^2 x_5 + (3 \cos^2 x_3 \cos^2 x_5 - 1)] \\ &\quad + Q_r / m_e \end{aligned}$$

$$\begin{aligned}
 x_3' &= x_4 \\
 x_4' &= -2(x_4 + 1)(x_2/x_1 - x_6 \tan x_5) - 1.5 \sin 2x_3 \\
 &\quad + Q_\theta/m_e x_1^2 \cos^2 x_5 \\
 x_5' &= x_6 \\
 x_6' &= -2x_6 x_2/x_1 - [0.5(x_4 + 1)^2 + 1.5 \cos^2 x_3] \sin 2x_5 \\
 &\quad + Q_\varphi/m_e x_1^2
 \end{aligned} \tag{21}$$

The general form of Equation (21) is

$$\frac{dx}{d\tau} = \mathbf{F}(\mathbf{x}, \mathbf{u}(\tau)) \tag{22}$$

where $\mathbf{F}(\mathbf{x}, \mathbf{u}(\tau))$ represents the vector function on the right part of the dynamic equations (21). $\mathbf{u}(\tau)$ is defined as a control function of the system. The control system has an input which is a tether electric current, and three outputs which are the distance r , in-plane angle θ , and out-of-plane angle φ .

A. LINEARIZED EQUATION

In the actual work of the control system, because of the unpredictable effect of various disturbances which will inevitably cause deviated from the equilibrium position of the vertical (the quasi-equilibrium position θ_1^*). Therefore, the working purpose of the control system is to reduce the deviation by relying on the current correction.

When the system is linear, that is

$$\frac{dy}{d\tau} = \mathbf{A}(\tau)y + \mathbf{M}(\tau)\Delta u \tag{23}$$

where the system state deviations are defined $\mathbf{y} = \Delta \mathbf{x} = (\Delta r, \Delta r', \Delta \theta, \Delta \theta', \Delta \varphi, \Delta \varphi')^T$, the matrix $\mathbf{A}(\tau)$ and $\mathbf{M}(\tau)$ are parameter matrixes. $\Delta u = \Delta I$ is control correction (scalar control), which can make the system to the desired state. The matrix $\mathbf{A}(\tau)$ and $\mathbf{M}(\tau)$ are given as follows, respectively

$$\mathbf{A}(\tau) = \begin{bmatrix} 0 & 1 & 0 & 0 & 0 & 0 \\ A_{21} & A_{22} & A_{23} & A_{24} & A_{25} & A_{26} \\ 0 & 0 & 0 & 1 & 0 & 0 \\ A_{41} & A_{42} & A_{43} & A_{44} & A_{45} & A_{46} \\ 0 & 0 & 0 & 0 & 0 & 1 \\ A_{61} & A_{62} & A_{63} & A_{64} & A_{65} & A_{66} \end{bmatrix}, \tag{24}$$

$$\mathbf{M}(\tau) = [0 \quad M1 \quad 0 \quad M2 \quad 0 \quad 0]^T$$

where $A_{kj} = \partial F_{r,\theta,\varphi} / \partial x_j$ is a Jacobian matrix which consists of the partial derivative of the state vector, k and j are both positive integers where $k = 1, \dots, 6, j = 1, \dots, 6$. The elements of the Jacobi matrix and control matrix are given in the appendix.

As can be seen from the linearized system in the quasi-equilibrium positions (14) are unstable.

B. CONTROLLABILITY

The controllability of the EDT system should be analyzed before the problem of dynamics control is solved. Gilbert's controllability criterion is adopted in this paper, which not only determines the controllability of the system itself but

determines what can be controlled and what cannot, the contents are as follows [27]. The criterion which requires the linear transformation $y = Vy_*$ to convert the linear system (23) to principal coordinates, where y_* denote principal coordinate vectors and V represent transformation matrix. The linear transformation of the system (23), as follows

$$\frac{dy_*}{d\tau} = D(\tau)y_* + M_*(\tau)\Delta u \tag{25}$$

where $D(\tau)$ is a diagonal matrix which is composed of the eigenvalues of the matrix $\mathbf{A}(\tau)$, $M_*(\tau) = V^{-1}M(\tau)$ is represent vector transformation of $M(\tau)$. If the matrix $M_*(\tau)$ is a column matrix (when the control Δu is a scalar), the controllability criterion requires that none of the components of the column be zero.

Besides, Kalman's controllability criterion can also be used to judge the controllability of the system [28]. This criterion is not intuitive, but it is more general because it is not restricted by the existence of multiple characteristic roots (or linear correlation vectors) in the system.

C. OPTIMAL CONTROLLERS

Controller synthesis that defined the relational expressions $u(y)$ between the controlled quantity and the system states. The standard procedure of the Bellman Dynamic Programming Principle (BDPP) is used for the synthesis of control in this paper. To obtain the optimal controllers, which ensure the quadratic optimal criterion minimum, that is

$$J = \int_0^{t_k} (y^T E y + h u^2) dt \tag{26}$$

where E is a diagonal positive definite weighting matrix, h is a weighting coefficient and $h > 0$, the matrices can be set and satisfy the constraint conditions $h + E_1 + E_2 + E_3 + E_4 = 1$. The main concerns of matrices E, h are a) to ensure efficient feedback weight on the parameters r, \dot{r} , which influence tether deformation; b) to ensure appropriate tracking of oscillation angle θ, φ and angular velocity $\dot{\theta}, \dot{\varphi}$. As far as the control issues are concerned, with small controlled quantity selected as much as possible make the system states converge to the quasi-equilibrium position. While all of the system states $\mathbf{y} = (\Delta r, \Delta r', \Delta \theta, \Delta \theta')^T$ are varies on a small scale, so whether on weight matrix or the corresponding weight coefficient of those states should not be too larger.

The optimal control Δu which minimizes the functional (26) is expressed as

$$\Delta u = p^T y \tag{27}$$

where $p = -GM/h$ is the coefficient of the optimal controller, the matrix G is defined by the Riccati Equation

$$GA + A^T G + E - GMM^T G/h = 0 \tag{28}$$

According to equation (28), it can be determined that matrix A should be a positive definite matrix. The equation (27) is written as

$$\Delta u_1 = p_0 \Delta \theta + p_1 \Delta \dot{\theta} + p_2 \Delta r + p_3 \Delta \dot{r} \tag{29}$$

The trial and error method is adopted to repeat the test in the course of the simulation, then the best control parameters are given.

The weight matrix is selected as

$$E_1 = 0.23, E_2 = 0.23, E_3 = 0.25, E_4 = 0.25, h = 0.04.$$

The optimum parameters of the controller are obtained as

$$p = [-3.4559 \ -3.2079 \ 3.2138 \ 3.6572]^T .$$

D. PID CONTROLLERS

Next, the PID structure is defined as:

$$\Delta u_2 = k_1(\Delta\theta + \Delta r) + k_2 \int_0^t (\Delta\theta + \Delta r)dt + k_3(\Delta\dot{\theta} + \Delta\dot{r}) \tag{30}$$

The parameters of the PID controller are selected as

$$k_1 = 3, \quad k_2 = 0.00001, \quad k_3 = 2.33.$$

V. SIMULATIONS RESULTS AND DISCUSSIONS

A reboost EDT system is applied to the following simulated analysis and the system parameters are given in Table 1. Supposing the EDT system is in an approximately circular orbit where the orbital inclination is 42 degrees and the orbital altitude is 400km (the current orbit of the Chinese Space Station). The nonlinear equations of motion are simulated using Mathcad with the initial conditions (shown in Table 1) and the following desired states:

$$y_{1d} = [2.99 \ 0]^T, \quad y_{2d} = [0 \ 0]^T, \quad y_{3d} = [5^0 \ 0]^T .$$

A. DYNAMICS OF THE UNCONTROLLED SYSTEM

As a benchmark for the effect of libration motion on the reboost EDT system boost process, the boost process without current control was studied first.

Figure 5 shows the time histories of tether chord length without current control and over a period of 10 and 100 orbits, respectively. As can be seen in Figure 5, the chord length is aperiodic oscillation and the libration is increased slowly with time because the Ampere force is regarded as distributed load act on the tether and the force is non-uniform which will cause tether deformation. The tether chord length phase plane is shown in Figure 6. It is clear from the figure that the tether chord is unstable.

The time histories of the in-plane angle are given in Figure 7. As demonstrated by Figure 7, the dynamics response of the in-plane angle is libration and non-periodic variations as time in 10 and 100 orbital periods, respectively, due to the time-varying disturbance of Ampere force. When the EDT system runs in orbit, the in-plane libration will gradually increase. The in-plane angle phase plane is demonstrated in Figure 8, it may be noticed that the in-plane angle is unstable.

Figure 9 depicts the histories of the out-of-plane angle. It can be found that the dynamics response of the out-of-plane

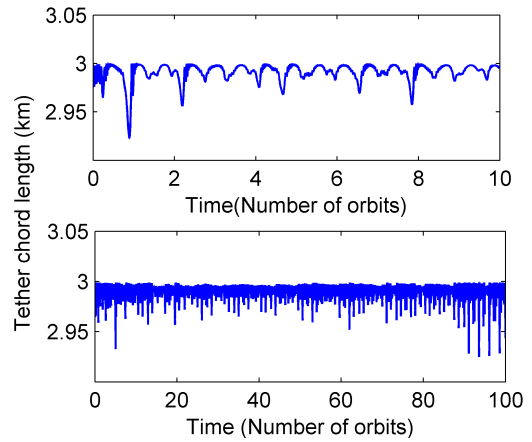


FIGURE 5. Time history of chord length without current regulation.

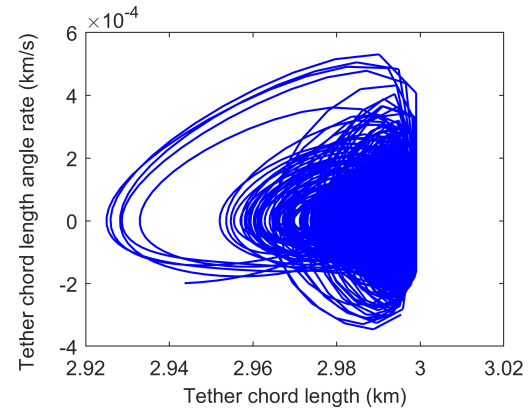


FIGURE 6. The tether chord length phase plane.

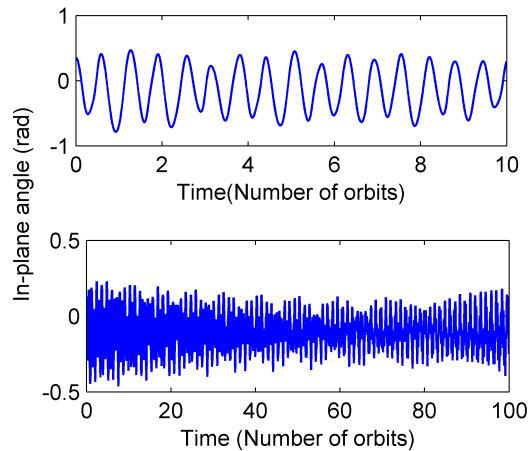


FIGURE 7. Time history of libration in-plane angle without current regulation.

angle becomes great gradually over time and the amplitude of the angle slowly becomes greater over long-time. The reason is that libration energy is inserted into the system, which is induced in-plane and out-of-plane motion by the nonlinear dynamic coupling. The out-of-plane angle phase plane is depicted in Figure 10. As seen from Figure 10, the out-of-plane angle gradually tended to a limit cycle.

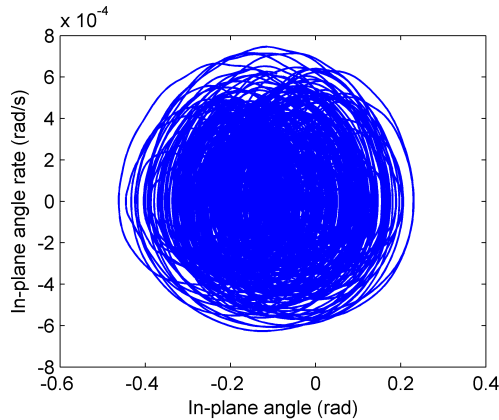


FIGURE 8. The in-plane angle phase plane.

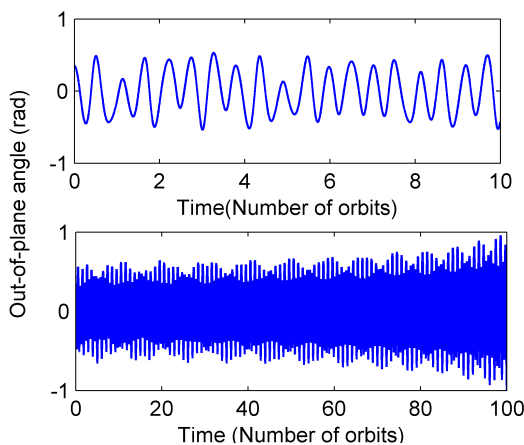


FIGURE 9. Time history of libration out-of-plane angle without current regulation.

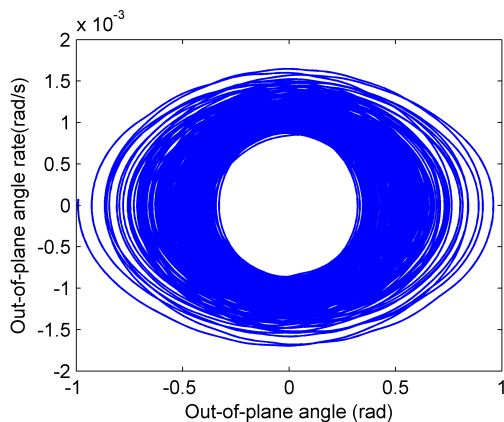


FIGURE 10. The out-of-plane angle phase plane.

B. REBOOST OF EDT SYSTEM WITH CURRENT CONTROL

The simulation results of the reboost EDT system are shown to evaluate the performance of the devised control laws for the three-dimensional libration problem. The effectiveness of the proposed BDPP control law is shown by comparing the control performance of the PID control method. It can be easy to see that the optimal control method is obviously superior to the PID control method in robustness and rapidity. terms

of convergence time and suppressing the libration motions to the EDT.

Figure 11 shows the time histories of tether chord length with current control, the solid red lines denote the tether chord in the quasi-equilibrium position. Compare Figures 5 and 11, it can be found that the chord length converged to the desired length of about 0.5 orbital periods. The chord length reached the desired value and remain stable without overshoot. It is clearly shown in Fig. 11 that the libration motion under the BDPP control law is less severe compared to the PID control law, due to BDPP has optimal properties, so it convergent with minimum cost.

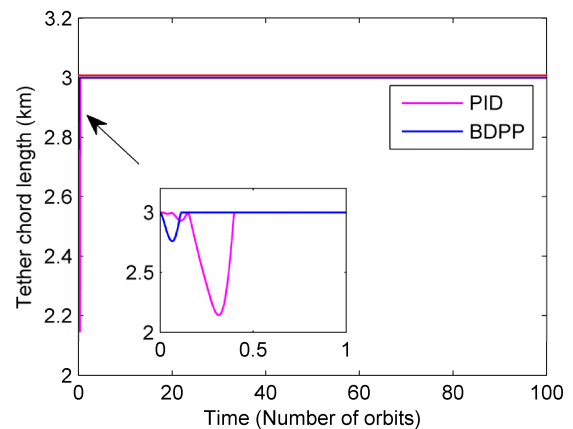


FIGURE 11. Variation curves of the tether chord length versus time.

The time histories of the in-plane angle are given in Figure 12. The solid red lines denote the in-plane angle in the quasi-equilibrium position. It is easy to find that the overshoot and settling time of the BDPP is distinct smaller than PID as for controlling the libration angles. By comparing Figure 7 with Figure 12, with the effect of the current controller, the in-plane angle rapidly converged to the desired quasi-equilibrium position in about two orbital periods with the two control laws. All of the control laws are still swings around the quasi-equilibrium position the result of the Ampere force is always acting on the tether.

Figure 13 depicts the time histories of the out-of-plane angle. As seen in Figure 13 there are some fluctuations in the curve of the out-of-plane angle at the first stage, then it is acted in small amplitude when the control current is decreased and it was converged to around 0^0 in three orbital periods with a swing around 2.3^0 . It can be seen in Figure 13 that the PID control law is vulnerable to the disturbance and suppress the libration motions of the EDT, whereas the short convergent time of the BDPP scheme results in a fast response. Despite the designed current controller is weak for out-of-plane motion, it can meet the requirement for the stability of the out-of-plane during the reboost process of the tether system.

Simulation results are shown in Figure 14 indicates that the tether tension is always positive and controlled near a stable value of 1.47N in about 2.5 orbital periods (as shown

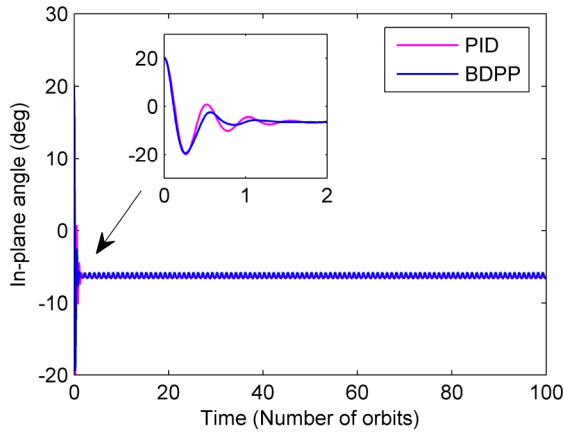


FIGURE 12. Variation curves of the in-plane angle versus time.

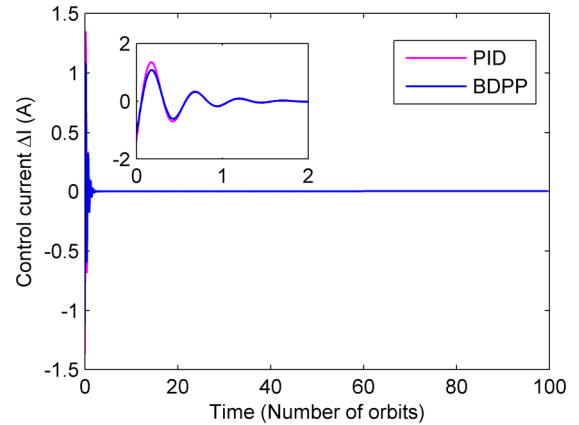


FIGURE 15. Variation curves of the control current versus time.

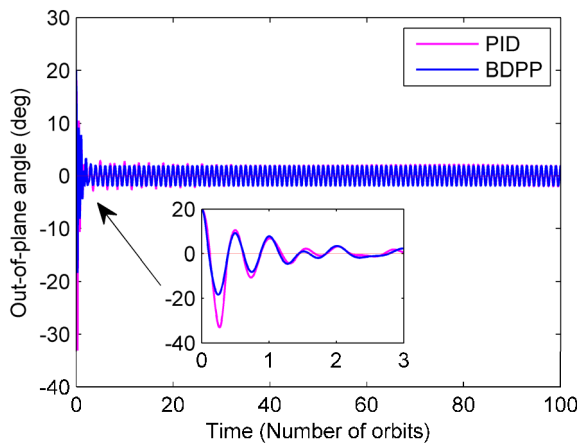


FIGURE 13. Variation curves of the out-of-plane angle versus time.

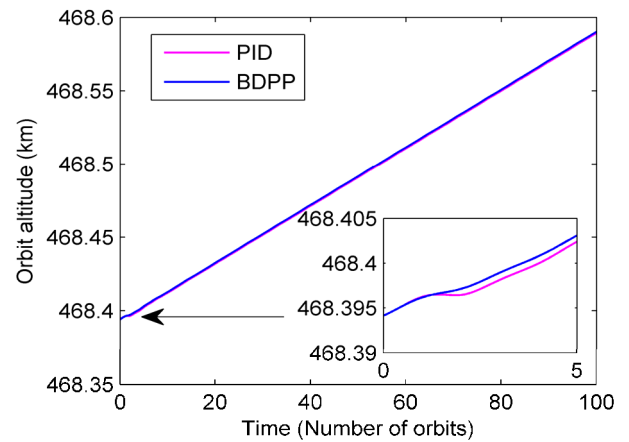


FIGURE 16. The orbit altitude of the center of EDT system.

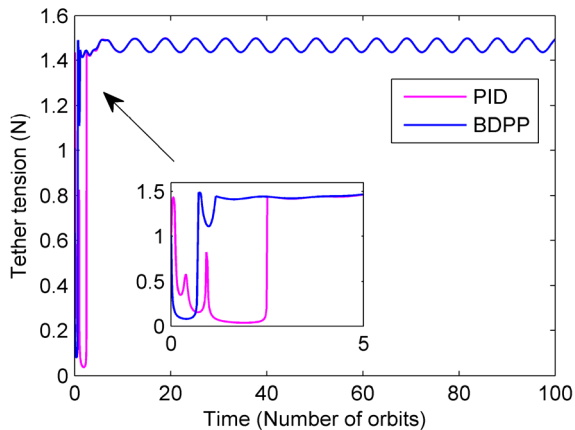


FIGURE 14. Variation curves of the tether tension versus time.

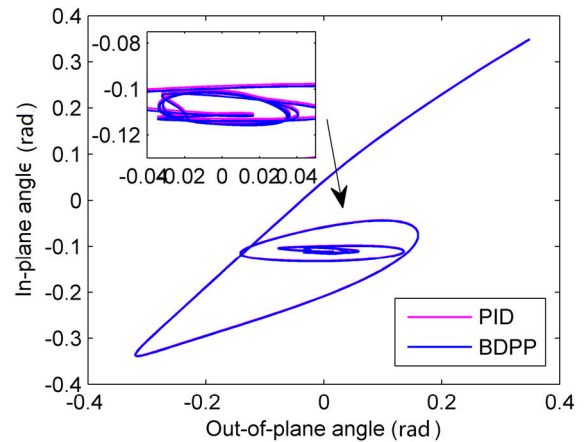


FIGURE 17. In-plane angle versus out-of-plane angle with current control.

in the inset). The explanation is that the tether is kept taut all the time and satisfied the physical requirement, which means that the EDT tether does not appear slack situation during the whole reboost process.

Figure 15 shows the time histories of the control current for both controllers. From the analysis of the simulation results, the BDPP made the respond speed faster and the overshoot less. At the initial moment, the tether and in-plane angle

vibrate violently, so the current regulation value is reached the maximum. The control current is converged to zero value in two orbital periods when the system state variables are trend to stable.

The main purpose of the paper is to boost the orbit altitude of the CSS. Figure 16 depicts the rise of the center of the EDT system in the orbit altitude. As shown, the rise in BDPP control is more than PID. The altitude rises about 200 and 190 meters in BDPP and PID in 100 orbital periods, respectively. The effectiveness and availability of the proposed controllers can be proved by synthesizing the above simulation results and analysis.

Figure 17 plots the in-plane angle versus the out-of-plane angle with the current control. It shows the control based on the BDPP and PID laws are effective. It can be concluded that the BDPP control law has better performance than the PID law in static and dynamic performances.

VI. CONCLUSION

This article investigated the dynamic analysis and libration control in reboost spacecraft utilizing EDT propulsion technology. The study is based on the hypothesis of a rigid tether and lumped mass on behalf of end bodies with their attitude neglected. Furthermore, the tether deformation is considered due to Ampere force (distributed load) act on the tether. The optimal controller based on Bellman dynamic programming principle and PID controller are presented to eliminate the tether deformation and libration motion. Simulation result analyses of the reboost EDT system shown that the current regulation is valid and the libration angles can be effectively confined to within a certain range to limit the EDT system from tumbling in the reboost process. By comparison, the BDPP controller can be better applied in the nonlinear system, with small overshoot, fast response and good applicability. The present study indicated that the optimal reboost efficiency by EDT would be achieved by control tether current through a properly designed control method. The combination of the above two methods is possible to achieve better effect in the future.

APPENDIX

The system matrix $\mathbf{A}(\tau)$ and control matrix \mathbf{M} are given

$$\mathbf{A}(\tau) = \begin{bmatrix} 0 & 1 & 0 & 0 & 0 & 0 \\ A_{21} & A_{22} & A_{23} & A_{24} & A_{25} & A_{26} \\ 0 & 0 & 0 & 1 & 0 & 0 \\ A_{41} & A_{42} & A_{43} & A_{44} & A_{45} & A_{46} \\ 0 & 0 & 0 & 0 & 0 & 1 \\ A_{61} & A_{62} & A_{63} & A_{64} & A_{65} & A_{66} \end{bmatrix},$$

$$\mathbf{M} = \begin{bmatrix} 0 & M_1 & 0 & M_2 & 0 & 0 \end{bmatrix}^T.$$

where $A_{ij} = \partial F_{r,\theta,\varphi} / \partial x_j$, $i = 1, \dots, 6$, $j = 1, \dots, 6$, $k \ni (\mathbf{r}, \theta, \varphi)$.

$$F_r = x_1[x_6^2 + (x_4 + 1)^2 \cos^2 x_5 + (3 \cos^2 x_3 \cos^2 x_5 - 1)] - B_0 I x_1 (\cot \psi \cos^2 x_5 + \sin^2 x_5 / \psi) / 2m_e \Omega^2,$$

$$F_\theta = -2(x_4 + 1)(x_2/x_1 - x_6 \tan x_5) - 1.5 \sin 2x_3 + B_0 I \Delta / m_e x_1.$$

$$F_\varphi = -2x_6 x_2/x_1 - [0.5(x_4 + 1)^2 + 1.5 \cos^2 x_3] \sin 2x_5 + B_0 I x_1^2 \sin x_5 \cos x_5 (\cot \psi - \psi^{-1}) / 2m_e x_1^2.$$

$$A_{21} = \frac{\partial F_r}{\partial x_1} = \cos^2 x_5 (x_4 + 1)^2 + x_6 + 3 \cos^2 x_5 \cos^2 x_3$$

$$- B_0 I (\cos^2 x_5 \cot \psi + \sin^2 x_5 / \psi) - 1$$

$$A_{22} = \frac{\partial F_r}{\partial x_2} = 0$$

$$A_{23} = \frac{\partial F_r}{\partial x_3} = -6x_1 \cos^2 x_5 \cos x_3 \sin x_3$$

$$A_{24} = \frac{\partial F_r}{\partial x_4} = 2x_1 \cos^2 x_5 (x_4 + 1)$$

$$A_{25} = \frac{\partial F_r}{\partial x_5} = -x_1 [2 \cos x_5 \sin x_5 (x_4 + 1)^2$$

$$+ 6 \cos^2 x_3 \sin x_5 \cos x_5]$$

$$+ B_0 I x_1 (2 \cos x_5 \cot \psi \sin x_5$$

$$- 2 \cos x_5 \sin x_5 \psi^{-1}) / 2m_e \Omega^2$$

$$A_{26} = \frac{\partial F_r}{\partial x_6} = 2x_1 x_6$$

$$A_{41} = \frac{\partial F_\theta}{\partial x_1} = 2x_2 (x_4 + 1) / x_1^2$$

$$A_{42} = \frac{\partial F_\theta}{\partial x_2} = -2(x_4 + 1) / x_1$$

$$A_{43} = \frac{\partial F_\theta}{\partial x_3} = -3 \cos(2x_3)$$

$$A_{44} = \frac{\partial F_\theta}{\partial x_4} = 2x_6 \tan x_5 - 2x_2 / x_1$$

$$A_{45} = \frac{\partial F_\theta}{\partial x_5} = 2x_6 (x_4 + 1) (\tan^2 x_5 + 1)$$

$$A_{46} = \frac{\partial F_\theta}{\partial x_6} = 2 \tan x_5 (x_4 + 1)$$

$$A_{61} = \frac{\partial F_\varphi}{\partial x_1} = 2x_2 x_6 / x_1^2$$

$$A_{62} = \frac{\partial F_\varphi}{\partial x_2} = -2x_6 / x_1$$

$$A_{63} = \frac{\partial F_\varphi}{\partial x_3} = 3 \sin 2x_5 \cos x_3 \sin x_3$$

$$A_{64} = \frac{\partial F_\varphi}{\partial x_4} = -\sin 2x_5 (x_4 + 1)$$

$$A_{65} = \frac{\partial F_\varphi}{\partial x_5} = \cos 2x_5 [-3 \cos^2 x_3 - (x_4 - 1)^2$$

$$+ B_0 I (\cot \psi - \psi^{-1}) / m_e \Omega^2]$$

$$+ B_0 I [\cos^2(x_5) - \sin^2(x_5)] (\cot(\psi) - \psi^{-1}) / 2\Omega^2 m_e$$

$$A_{66} = \frac{\partial F_\varphi}{\partial x_6} = -2x_2 x_1$$

$$M_1 = B_0 x_1 \cot \psi / 2m_e \Omega^2, M_2 = B_0 \Delta / x_1 m_e \Omega^2.$$

REFERENCES

- [1] P. Tortora, "A low-cost mission for testing in-orbit a passive electrodynamic tether de-orbiting system," in *Proc. Spaceflight Mech.*, 2004, pp. 1–3.
- [2] H. Cai, Y. W. Yang, and C. F. Guo, "Review of electrodynamic tether system," *Yuhang Xuebao/J. Astronaut.*, vol. 11, no. 35, pp. 1223–1232, 2014.
- [3] H. Lu, Y. M. Zabolotnov, and A. Li, "Application of spinning electrodynamic tether system in changing system orbital parameters," *J. Phys., Conf. Ser.*, vol. 1368, Nov. 2019, Art. no. 042002.

- [4] P. S. Voevodin and Y. M. Zabolotnov, "Stabilizing the motion of a low-orbit electrodynamic tether system," *J. Comput. Syst. Sci. Int.*, vol. 58, no. 2, pp. 270–285, Mar. 2019.
- [5] J. Huang, "Current and tension control for deployment of a deorbiting electro-dynamic tether system," *Hangkong Xuebao/Acta Aeronautica Astronautica Sinica*, vol. 39, no. 2, 2018, Art. no. 321464.
- [6] J. Liu, G. Li, Z. H. Zhu, M. Liu, and X. Zhan, "Automatic orbital maneuver for mega-constellations maintenance with electrodynamic tethers," *Aerosp. Sci. Technol.*, vol. 105, Oct. 2020, Art. no. 105910.
- [7] J. Bonometti, "Free re-boost electrodynamic tether for the international space station," in *Proc. 41st AIAA/ASME/SAE/ASEE Joint Propuls. Conf. Exhib.*, 2005, p. 4545.
- [8] L. Johnson, "Propulsion and power using electrodynamic," in *Proc. Planetary Science Vision Workshop*, 2017, pp. 1–5.
- [9] H. Kojima and T. Sugimoto, "Stability analysis of in-plane and out-of-plane periodic motions of electrodynamic tether system in inclined elliptic orbit," *Acta Astronautica*, vol. 65, nos. 3–4, pp. 477–488, Aug. 2009.
- [10] G. Li, Z. H. Zhu, and S. A. Meguid, "Libration and transverse dynamic stability control of flexible bare electrodynamic tether systems in satellite deorbit," *Aerosp. Sci. Technol.*, vol. 49, pp. 112–129, Feb. 2016.
- [11] P. S. Voevodin and Y. M. Zabolotnov, "Modeling and analysis of oscillations of electrodynamic tether system on orbit of Earth satellite," *Matematicheskoe Modelirovanie*, vol. 29, no. 6, pp. 21–34, 2017.
- [12] A. A. Tikhonov, "A control method for angular stabilization of an electrodynamic tether system," *Autom. Remote Control*, vol. 81, no. 2, pp. 269–286, Feb. 2020.
- [13] D. Xu and X. Kong, "Tether modeling study on electro-dynamic tether deorbiting system," *Acta Aeronautica Astronautica Sinica*, vol. 29, pp. 1196–1201, 2008.
- [14] J. Liu, G. Li, Z. H. Zhu, and X. Zhan, "Orbital boost characteristics of spacecraft by electrodynamic tethers with consideration of electric-magnetic-dynamic energy coupling," *Acta Astronautica*, vol. 171, pp. 196–207, Jun. 2020.
- [15] J. Liu, X. Zhan, G. Li, Q. Wang, and S. Wang, "Dynamics of orbital boost maneuver of low Earth orbit satellites by electrodynamic tethers," *Aerosp. Syst.*, vol. 3, no. 3, pp. 189–196, Sep. 2020.
- [16] J. Pelaez and E. C. Lorenzini, "Libration control of electrodynamic tethers in inclined orbit," *J. Guid., Control, Dyn.*, vol. 28, no. 2, pp. 269–279, Mar. 2005.
- [17] M. Iñarrea and J. Peláez, "Libration control of electrodynamic tethers using the extended time-delayed autosynchronization method," *J. Guid., Control, Dyn.*, vol. 33, no. 3, pp. 923–933, May 2010.
- [18] P. Williams, "Libration control of electrodynamic tethers using predictive control with time-delayed feedback," *J. Guid., Control, Dyn.*, vol. 32, no. 4, pp. 1254–1268, Jul. 2009.
- [19] Y.-W. Yang and H. Cai, "Extended time-delay autosynchronization method for libration control of electrodynamic tether using lorentz force," *Acta Astronautica*, vol. 159, pp. 179–188, Jun. 2019.
- [20] R. Zhong and Z. H. Zhu, "Libration dynamics and stability of electrodynamic tethers in satellite deorbit," *Celestial Mech. Dyn. Astron.*, vol. 116, no. 3, pp. 279–298, Jul. 2013.
- [21] C. Luo, H. Wen, and D. Jin, "Libration control of bare electrodynamic tether for three-dimensional deployment," *Astrodynamics*, vol. 2, no. 3, pp. 187–198, 2018.
- [22] S. Chen, A. Li, C. Wang, and C. Liu, "Adaptive sliding mode control for deployment of electro-dynamic tether via limited tension and current," *Acta Astronautica*, vol. 177, pp. 842–852, Dec. 2020.
- [23] G. Li, Z. H. Zhu, J. Cain, F. Newland, and A. Czekanski, "Libration control of bare electrodynamic tethers considering elastic-thermal-electrical coupling," *J. Guid., Control, Dyn.*, vol. 39, no. 3, pp. 642–654, Mar. 2016.
- [24] A. A. Tikhonov, "On damping of the oscillations of electrodynamic tether system," in *Proc. Academic Space Conf.*, 2019, pp. 1–5, doi: 10.1063/1.5133205.
- [25] V. V. Beletsky and E. M. Levin, *Dynamics of Space Tether Systems*, vol. 83. American Astronautical Society, 1993, pp. 272–274.
- [26] P. S. Voevodin and Y. M. Zabolotnov, "Analysis of the dynamics and choice of parameters of an electrodynamic space tether system in the thrust generation mode," *Cosmic Res.*, vol. 58, no. 1, pp. 42–52, Jan. 2020.
- [27] E. M. Levin, *Dynamic Analysis of Space Tether Missions* (Advances in the Astronautical Sciences), 2007, p. 126.
- [28] C. A. Antoulas, "Kalman's controllability rank condition: From linear to nonlinear," in *Mathematical System Theory*. 1991, ch. 25, pp. 453–462, doi: 10.1007/978-3-662-08546-2.



YANFANG LI was born in Shaanxi, China. She received the B.E. degree from the School of Electronics and Information Engineering, Xi'an Technological University, Xi'an, China, in 2010, and the M.E. degree from Xi'an Technological University, in 2013. She is currently pursuing the Ph.D. degree with the School of Automation, Northwestern Polytechnical University, Xi'an. From September 2013 to March 2017, she has been an Experimenter with the Energy Engineering College, Yulin University. Her scientific work is focused on dynamic and control of space tether systems and this work led to the Ph.D. degree.



AIJUN LI was born in Heilongjiang, China. He received the B.E. degree in aircraft design, the M.E. degree in navigation, guide, and control, and the Ph.D. degree in pattern recognition and intelligent systems from the School of Automation, Northwestern Polytechnical University, in 1995, 2000, and 2005, respectively.

From December 2000 to April 2006, he was a Lecturer and from April 2006 to March 2011, he has been an Assistant Professor. Since

April 2011, he has been a Professor and an Advisor for the Ph.D. students with the School of Automation, Northwestern Polytechnical University, Xi'an, China. He has published several articles in international journals, conferences papers, and book chapters. He has been involved in several projects. His research interests include flight control and simulation, intelligent control, and dynamic and control of space tether systems.



CHANGQING WANG received the B.E. degree in mechanism design and automation and the M.E. degree in guidance, navigation and control from Northwestern Polytechnical University, in 1996 and 2001, respectively, and the Ph.D. degree in system analysis, control and information processing from the Moscow Power Engineering Institute, in 2006. From 1996 to 2003, he was a Research Assistant with the School of Mechatronics. From 2003 to 2011, he was a Lecturer with the

School of Mechatronics and the School of Automation. From 2011 to 2020, he has been an Assistant Professor with the School of Automation. Since June 2020, he has been a Professor and an Advisor for Ph.D. students with the School of Automation, Northwestern Polytechnical University, Xi'an, China. He is the author of several books, articles, and inventions. He has been taken part in several projects. His research interests include flight control and simulation and dynamic and control of space tether systems.



HAOCHANG TIAN was born in Hebei, China. He received the B.E. degree from the School of Automation, Northwestern Polytechnical University, Xi'an, China, in 2016, and the M.E. degree from Northwestern Polytechnical University, in 2018, where he is currently pursuing the Ph.D. degree with the School of Automation. His scientific work is focused on dynamic and control of space tether systems.

• • •